Shallow-water circulation on the northern coast of Rio Grande do Sul, Brazil: A wave-dominated system

Mauro Michelena Andrade [a],[*], Elírio E. Toldo Jr. [a], Pedro Veras Guimarães [b],[c], Nicolas de Assis Bose [a]

[a] Programa de Pós-Graduação em Geociências, Instituto de Geociências, Universidade Federal do Rio Grande do Sul, Av. Bento Gonçalves, 9500, Porto Alegre, RS, 91501-970, Brazil
[b] France Énergie Marines (FEM), 525 Avenue Alexis de Rochon, Plouzanè, 29280, France
[c] Programa de Pós-Graduação em Oceanografia, Instituto de Oceanografia, Universidade Federal de Santa Catarina, Rua Eng., Agrônomo Andrey Cristian Ferreira, Florianópolis, SC, 88040-900, Brazil

ABSTRACT

Alongshore currents in the surf zone are formed after incident waves break. This process depends on the characteristics of the incident waves and can be altered by the wind, and to a lesser extent, by bathymetry and tide. In order to understand the behavior of the alongshore currents on the north coast of Rio Grande do Sul (Brazil), two datasets were obtained in the field. The first one was acquired during oceanographic moorings and is composed of long time series of wave data. The other database corresponded to direct measurements of vertical profiles of velocities and direction of alongshore currents in the surf zone, both simultaneously acquired for the first time in this coastal region. The analyses of these data sets enabled identification and quantification of the processes associated with incident waves and winds. Circulation by currents in the surf zone is induced by oblique incidence waves breaking as a result of radiation-stress energy flow. It was also noted that wind can influence alongshore currents to a lesser extent. The findings indicated that height and angle of incidence of waves was the main driving force of alongshore currents. A pattern has also been identified, in which waves that come from the southeast (SE) and northeast (NE) generate northeasterly and southwesterly fluxes, respectively.

© 2021 Elsevier B.V. All rights reserved.

1. Introduction

When waves approach shallow-water regions, they are susceptible to transformations due to water depth gradients, like reflection, refraction, shear stress, and breaking (Holthuijsen, 2010). An important mechanism associated with the oblique angle at which waves approach the coastline occurs at the moment of wave breaking. This process produces an energy vector that drives an alongshore current within the surf zone (Davis and FitzGerald, 2009). It always takes place when the incidence of waves is oblique in relation to the shoreline, and is mainly controlled by the height and angle of wave incidence. This energy vector is defined as a radiation-stress flow that may be transverse to the wave-propagation movement (Longuet-Higgins, 1970, In: Komar, 1976) and drives the alongshore current. However, these currents can coexist with tide- and wind-driven currents (Nielsen,

2009). Alongshore current driven by radiation stress is particular to each environment and it also depends on the bottom slope as well as the height and angle of wave incidence (Longuet-Higgins, 1970).

This process could result in a dynamic pattern of coastal circulation, which is fundamental for the sediment budget on the coast (van Rijn, 1993). In the surf zone, this is an extremely dynamic process responsible for transporting the sediments reworked by the turbulence of wave breaking, and which are both in suspension and on the bottom, through long distances (Araújo and Alfredini, 2001; U. S. Army, 1984). Shoreline management requires information regarding nearshore hydrodynamics and longshore sediment transport to design schemes to protect the coastline (George et al., 2019). Understanding these mechanisms along a coast is one of the most basic required tasks in coastal engineering and is crucial for developing projects, coastal management plans, and erosion risk analyses (Pilkey and Cooper, 2014; Trombetta et al., 2020).

This highlights the importance of understanding the sediment balance and the need to study the processes associated with these events. These kinds of studies could support technical solutions

* Correspondence to: Programa de Pós-Graduação em Ciência e Tecnologia Ambiental, Escola do Mar Ciência e Tecnologia, Universidade do Vale do Itajaí. Rua Uruguai, 458, Itajaí, SC, 88302-901, Brazil.
E-mail address: mauromichelena@gmal.com (M.M. Andrade).

for the preservation of densely occupied areas. Reinforcing this point, the relative role of the different physical processes and their coupling as a force that drives sediment transport across the continental shelf remains poorly understood in some regions. This is due to the lack of simultaneous field observations at different depths (Torres-Freyermuth et al., 2017).

Furthermore, there is a significant upward trend in the mean sea level at various points around the world – including sites on the Brazilian coast (PBMC, 2016) – as well as an intensification of extreme events of positive sea level anomaly (Neves Filho, 1992; Mawdsley et al., 2014). These effects would be more damaging if the height and duration of storms increased as a result of climate change as demonstrated in Fiore et al. (2009). In this scenario, coastal regions around the world should, in general, become more vulnerable (Cartier et al., 2013).

The coast of the state of Rio Grande do Sul (RS) is an example of an area highly vulnerable to mean sea level rise in the future due to its intrinsic morphodynamic characteristics, such as its low coastal gradient combined with a high degree of exposure to oceanic dynamics (Germani et al., 2015; Guimarães et al., 2015). Moreover, some processes associated with hydrodynamics and the intensification of extreme events of positive sea level anomaly (Neves Filho, 1992, Mawdsley et al., 2014) can affect the local geomorphology and sediment movement representing coastal hazards and risks along the state's coastline. The risks imply coastal erosion, habitat loss, and environmental changes. The hazards are related to major accidents that could happen with coastal users, including fatalities (Calliari et al., 2010).

Over the last six decades on the RS coast, several studies have been carried out on coastal currents and sediment transport (Motta, 1964, 1967; Pitombeira, 1975; Tomazelli and Villwock, 1992; Toldo et al., 1993; Lima et al., 2001; Lélis and Calliari, 2003; Toldo and Almeida, 2003; D'Aquino, 2004; Toldo et al., 2006a; Jung and Toldo, 2011, 2012; Motta et al., 2015; Silva and Toldo, 2017; Schossler et al., 2017; Sprovieri, 2018). These studies used several methodologies ranging from the most empirical – applying drifters and chronometers – to the most sophisticated— using oceanographic instrumentation and numerical computational modeling. Studies by Motta et al. (2015) and Sprovieri (2018) that used numerical modeling to explore the relationship between wave incidence and sediment transported stand out.

However, no study has attempted to explain the dynamic process of coastal currents on the RS coast. The lack of a modern methodology to quantitatively observe such processes was also noticed. Besides, divergences in the results concerning the direction of the alongshore current – especially in the first conducted research works – raise uncertainties, and some questions even arise from the most recent above cited works: can the applied techniques or the analyzed periods have yielded wrong results and conclusions? Can the regional anthropogenic activities and global climate change be changing wave patterns and consequently the magnitude and direction of alongshore currents?

Research works using suitable equipment and methodology for the observations of incident waves and vertical profiles of current speed and direction in the surf zone are scarce (Villas-Boas et al., 2019). Furthermore, the study and acquisition of long time-series of simultaneous data regarding the driving forces to be compared with the alongshore currents are rare not only in the study area, but in the whole world (Torres-Freyermuth et al., 2017). Waves are the main force responsible for the alongshore currents and sediment transport in the surf zone of this coast (Dillenburg et al., 2004; Calliari and Toldo, 2016). Therefore, for a better understanding of physical processes between incident waves and currents in the surf zone of the northern RS coast, simultaneous observations must be made.

In this context, the main objective of the present work is to relate observations of alongshore currents measured in the surf zone to their main driving forces in shallow waters: waves and winds. With that, the present authors intend to improve the understanding of coastal drift hydrodynamics and also develop a basic conceptual model for shallow-water circulation for the northern RS coast, an environment that presents great complexity.

1.1. Study area

The South Brazilian Continental Shelf (SBCS), located between Cape Santa Marta (29° S) and Chuí (34° S), extends until the 180-m isobath and is 110 km and 170 km wide in the northern and southern portions, respectively (Calliari et al., 2009; Hartmann, 1996). The bottom slope is between 0.03° and 0.08°, which is considered mild (Toldo et al., 2006a). The RS coastline is approximately 620 km long and has a northeast-southwest orientation, without bays or promontory, and has only two permanent discontinuities: the mouths of the Patos and Tramandaí lagoons. This continuous barrier is characterized by sandy oceanic beaches that are between 50 and 100 meters wide with slopes between 3° and 5° (Dillenburg et al., 2004).

The precise location of the study area is the nearshore, and the surf zone off Tramandaí city on the northern portion of the RS coastline (Fig. 1). This part of the coast makes a regional angle of 20° relative to True North. The foreshore is broad and shallow and has an outer boundary between 10 and 15 m deep (Toldo et al., 2006b). Tramandaí beach presents a low gradient and varies between intermediate to dissipative, mostly having two or more wave breaking lines. Large sandbars are arranged along the shore in a bar-trough structure (Toldo et al., 2006b). The bottom consists of well-sorted fine sandy sediments.

The studies from Zavialov et al. (2002), Costa and Möller (2011), and Andrade et al. (2016) reported a wind-driven circulation of currents on the continental and inner-shelf that was influenced by the passage of meteorological systems. Predominantly barotropic low-frequency flows were also verified, presenting residual currents to the NE or SW whose directions depended on the season. Another oceanographic process identified on the RS coast was the so-called upwelling and downwelling near the coast (Andrade et al., 2016).

The astronomical tide on Tramandaí beach is mixed with a semi-diurnal predominance and is classified under a microtidal regime, with a mean amplitude of 0.31 m and a maximum height of 0.96 m (Andrade et al., 2018). However, when the maximum amplitudes driven by meteorological and astronomical forces were added, values higher than 1.2 m above the mean sea level were recorded without considering the wave run-up effects (Andrade et al., 2018).

Regarding the wind regime, northeasterly winds prevail throughout the year, but periodic reversals to the SW direction are observed during the passage of meteorological systems, which are more frequent in the fall and winter (Cavalcanti and Kousky, 2009). Previous studies (Barros et al., 2002; Piola et al., 2005) showed that the wind field also presents a large interannual variability associated with El Niño—Southern Oscillation events.

Swell waves reaching the shore on the northern RS coast are generated in the south of the Atlantic Ocean at around 60° of latitude. Sea waves from the northeast (NE) are driven by the local wind that prevails in the summer and spring. The wave climate is characterized by waves with significant heights of 1.5 m and periods between 7 and 9 s (Strauch et al., 2009), except during the passage of meteorological systems when much higher waves are recorded. Motta et al. (2015) identified a seasonality in the direction of coastal sediment drift associated with wave incidence
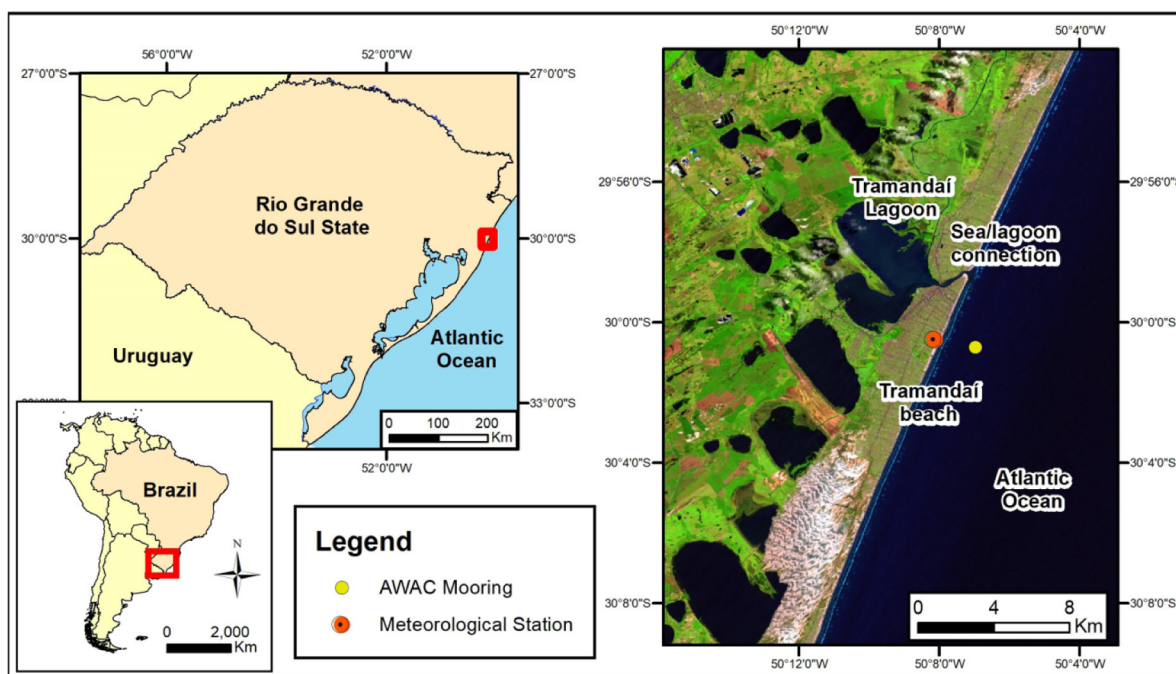
Fig. 1. Location of the coastal zone from the northern portion of the state of Rio Grande do Sul (RS) and Tramandaí beach. Yellow and red circles represent the location of the AWAC mooring and the meteorological station, respectively. (For interpretation of the references to colour in this figure legend, the reader is referred to the web version of this article.)

angles, using wave data and WAVEWATCH III numerical model results.

One of the pioneering pieces of research on the measurement of current velocities in the surf zone using an acoustic doppler current profiler (ADCP) was performed by Jung and Toldo (2011). These authors described an interaction between the wave climate (visually estimated) and the circulation inside the surf zone. They reported bidirectionality of the longitudinal currents and also great variability in the intensity of the currents in the Tramandaí beach region. In the same region but using a database of only alongshore surface current directions (observed visually once a day for 4 years), Jung and Toldo (2012) found seasonality in the direction of the current. In the summer and spring months, the flow was southwestward, while in the winter and fall, northeastward currents predominated. However, an annual bidirectional pattern with no predominance was identified, i.e., the annual resulting coastal drift can be towards the SW, or NE (Nicolodi et al., 2000). Still using this data of surface currents, a correlation between the direction of wave incidence and the alongshore current was identified.

2. Material and methods

In 2013, the nearly uninterrupted monitoring of waves, currents, sea level, and water temperature by oceanographic moorings off Tramandaí beach commenced. Furthermore, a new methodology for the acquisition of vertical profiles of current speeds and direction within the surf zone began to be used. It should be highlighted that this is the first time that long and consistent time series and also appropriate equipment for measurements were available to this region.

The methodology used in the acquisition of the data will be described in Section 2.1, where wave parameters correspond to time series recorded on the nearshore at 14 m deep; the WAVEWATCH III model (hereinafter abbreviated as WW3) describes how the time series were supplemented by the results from numerical simulations performed when data gaps in the measured data

Table 1
Sampling periods, season, and mooring depth of the oceanographic moorings located at Tramandaí beach.

Mooring	Start date	End date	Season	Depth (m)
#1	12/17/2013	03/13/2014	Summer	12
#2	06/24/2014	04/27/2015	Winter/Spring/Summer	12
#3	04/27/2015	07/30/2015	Autumn	14
#4	01/19/2016	06/21/2016	Summer/Autumn	14
#5	05/06/2017	09/08/2017	Autumn/ Winter	14

time series were observed; the wind data was measured by the weather station; and the procedures for measuring longitudinal currents are outlined. Data processing, validation of the WW3 model, and the performed analyses between the wave data and the alongshore current are presented in Section 2.2.

2.1. Data acquisition

2.1.1. Wave data

The wave data used in this work was acquired from five mooring campaigns between December 17, 2013 and September 8, 2017 (Table 1). The same instrument was installed on each mooring, which was an acoustic waves and currents profiler (1-MHz Nortek/AWAC). These moorings acquired all the wave parameters; however, analyses were restricted to the following variables: significant wave height (Hs), peak period (Tp), and mean direction (Dir). The vertical profiles of currents and sea level oscillations were also measured and the results are published in Andrade et al. (2016, 2018). On the first two moorings, the instrument was installed at 12 m of depth and on the last three, 14 m. The distance between those two sites was not greater than 400 m.

The initial estimation of the battery life for mooring #5 was 6 months (until November 2017), however, the battery ran out before that (in September 2017). This made it impossible to compare the wave data with the alongshore current data measured in the surf zone during September and October. Therefore, only for
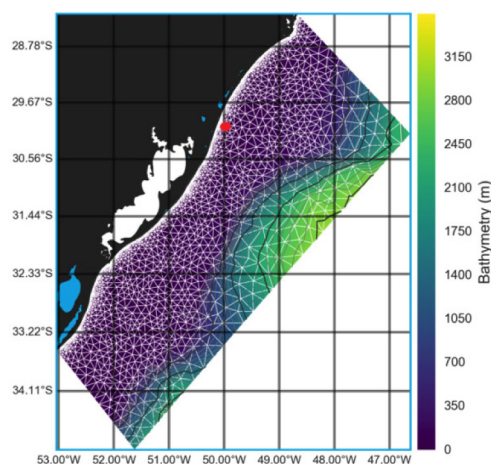
Fig. 2. Unstructured grid with the respective SBCS bathymetry. The spatial resolution of the domain increases as the depth decreases. Red circle represent location of the AWAC mooring and data extraction point.

this condition, the results from WW3 numerical simulations were used. The numerical approach used to fill this gap is described below.

2.1.2. WW3 model

The third-generation WAVEWATCH III model (Tolman, 2009), version 5.16, was used to generate wave data for the two periods in which there were no AWAC measurements. This model has been extensively used to perform hindcasting on global and regional scales (Chawla et al., 2013; Rascle and Ardhuin, 2013; Durrant et al., 2014).

The simulations were performed using the advection schemes over an unstructured grid, implemented by Roland (2008), and the source functions for wave dissipation and generation followed the ones used in reference test case "TEST471" from Ardhuin et al. (2010). The nonlinear wave interactions were modeled using Discrete Interaction Approximation (DIA, Hasselmann et al., 1985). The simulations were made using a high-resolution triangular mesh that covers the entire SBCS. This mesh scheme allows a more refined resolution towards the coast, reaching up to approximately 700 m from the coastline (Fig. 2). With that, it was possible to optimize the wave model execution time in the open ocean and at the same time have better discretization of the bathymetric grid and wavefield in shallow and intermediate waters, without losing information by grid nesting. The bathymetric database used for this mesh was the same as Guimarães et al. (2015), which in shallow and intermediate waters is composed by a set of observational data extracted from nautical charts.

The spectral boundary condition came hourly from another $0.5° \times 0.5°$ global WW3 simulation, also performed using the same Ardhuin et al. (2010) parameterization. Both global and regional grid simulations were forced by the same wind field used in the reanalysis project from the European Center for Medium-Range Weather Forecasts (ECMWF) forecasting center, generated in a $0.75° \times 0.75°$ spatial resolution grid every 3 h. The global simulation was also forced with an ice concentration mask (Tolman, 2003) with a $0.5° \times 0.5°$ resolution updated daily from the National Center for Environmental Prediction (NCEP, Kalnay et al., 1996).

2.1.3. Alongshore current measurements in the surf zone

To measure the alongshore currents between sandbars in the surf zone, the Tramandaí fishing platform was used. It is 350 m long, 8 m wide, and is a T-shaped pier facing seaward. The

Table 2
Periods of the field campaigns of alongshore current measurements carried out from the Tramandaí fishing platform. The season of the field campaign and the wave data source is also shown.

Campaign	Start date	End date	Season	Data source
#1	12/05/2014	12/06/2014	Spring	AWAC
#2	05/12/2015	05/13/2015	Autumn	AWAC
#3	01/28/2016	01/28/2016	Summer	AWAC
#4	05/05/2016	05/06/2016	Autumn	AWAC
#5	09/19/2017	09/24/2017	Winter	WW3
#6	10/14/2017	10/16/2017	Spring	WW3

data regarding alongshore current velocity and direction was acquired on six field campaigns during the same period as the moorings (Table 2). A 1-MHz Nortek Aquadopp current profiler with a right-angle head was used. It was configured to measure vertical profiles with 0.5 m cells. Vertical speed profiles were continuously measured every 10 s during short bottom moorings lasting 10 min. Measurements of the current in the channel were taken at the same instant as the moored AWAC wave measurements, i.e., every 3 h during daytime periods in campaigns that lasted from one to four days. The location of these measurements was 1.5 km away from the AWAC mooring site described in Section 2.1.1.

The Aquadopp was lowered from the side of the fishing platform that was exposed to incoming waves by strings, until reaching the bottom, to be positioned in the region between sandbars, i.e., in the alongshore channel in the surf zone. The location of this channel was defined by bathymetry performed with a plumb line during each campaign. The surf zone topographic profiles were measured with the help of a GPS system, from the shoreline to the end of the fishing platform, every 20 m. An example of the topographic profiles (depth) and the site that the Aquadopp was positioned is presented in Fig. 3.

2.1.4. Wind data

The wind direction and intensity were sampled by a *Vaisala* MAWS 301 automatic weather station that was installed and maintained by the Brazilian National Institute of Meteorology (INMET). The station was located on land at a little more than 500 m away from the Tramandaí fishing platform in an obstacle-free area. The weather station was positioned at 10 m above the ground. The data was sampled every minute and integrated into an hourly time interval.

2.2. Data treatment

The first step in processing the AWAC and Aquadopp data was the evaluation of data quality using the Storm software from Nortek. In this step, the angle of the sensors in relation to the bottom was verified. The magnetic declination was added to correct the orientation of wave direction data. The relationship between the acoustic signal and the signal-to-noise ratio was checked.

The files – generated by Storm in a text format – containing the wave parameters (Hs, Dir, and Tp) measured by the AWAC, and the current speed and direction measured by the Aquadopp, were imported into mathematical programs for analysis. In this step, the data consistency was verified and the spikes were eliminated. For example, the data sampled when the Aquadopp inclined higher than 20° was also excluded since large angles cannot be corrected (NORTEK, 2013). Finally, the same time periods corresponding to the alongshore current measurements in the channel and wave data were selected.

With the Aquadopp data, the mean profile was calculated and the intensity of the alongshore current velocity was determined
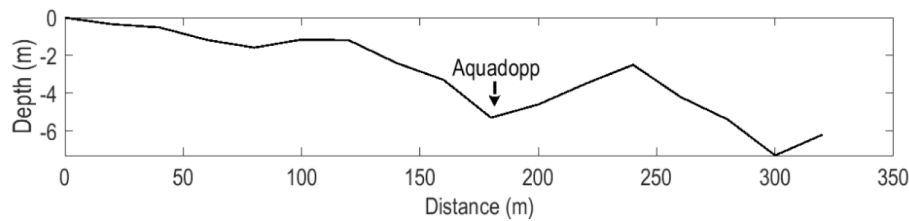
Fig. 3. Bathymetric profile of the September 19, 2017 campaign. The arrow indicates the point at which the instrument was placed for measurements.

Table 3
Mean square error (RMSE), Pearson's correlation coefficient®, and bias calculated between the AWAC data and the WW3 results.

	RMSE	R	Bias
Hs [m]	0.30	0.90	−0.0068
Tp [s]	0.76	0.76	−1.03
Dir [°]	8.56	0.94	−2.35

by the mean of each mean profile. These mean values were calculated based on a complete measurement, i.e., a 10-minute mean of the current intensity with sampling frequency of 10 s The current directions were obtained by calculating the mode of the directions. These procedures were followed due to significant turbulence in the surf zone.

2.2.1. WW3 validation with the AWAC data

The model results generated for the same location as the AWAC mooring were validated using the 4-month data that the instrument recorded on Mooring #5. The objective was to reconstitute the sea state conditions for the period between Sep. 8, 2017 and Oct. 10, 2017, in which the AWAC ran out of battery. The comparison between observed and simulated data of significant wave height (Hs, Fig. 4a), peak period (Tp, Fig. 4b), and mean direction (Dir, Fig. 4c) indicated that the model mostly satisfactorily reproduced the main wave parameters in the region under study.

The simulated and observed values were statistically compared to validate and quantify the difference between them. For this purpose, the mean square error (RMSE), Pearson's correlation coefficient (R), and bias were calculated. These statistical variables are widely used by several authors for model validation (Perignon, 2017; Guimarães et al., 2015; Ardhuin et al., 2010; Melo et al., 2008). Table 3 presents the validation of the parameters Hs, Tp, and Dir using the statistical variables mentioned above. In general, the model presented low variability of the results when compared to the AWAC data.

2.2.2. Wave and current analyses

The waves parameters (Hs, Tp, and Dir) recorded by the AWAC on the inner continental shelf and generated by the numerical model (at the same place) were selected to be transformed into a theta angle by subtracting 110°. Of this value, 20° corresponds to the slope of the coast in relation to true north, and 90° to the complementary angle. Thus, the angle between the wave radius and the parallel depth contours that were to be used below was obtained.

Snell's law was used to account for the change in direction caused by the wave refraction from the AWAC point to the breaking point of the wave, which has a typical horizontal distance of approximately 1000 m. As the two points are considered to be shallow water, the phase speed in shallow waters ($C = \sqrt{g.d}$) was considered. For this, the depth (d) at the break point was obtained through an approximation, in which it can be considered that the wave breaks when the ratio of wave height (Hs) to local depth is greater than 0.75 (Holthuijsen, 2010). However, due to the low

slope between the two points, the wave height at the break point that may be altered by shoaling has not been corrected.

Using the methodology proposed by Nielsen (2009), the momentum flux (F_m) along the coast was calculated using Eq. (1):

$$Fm = \rho g H_b^2 sin2\alpha_b \qquad (1)$$

where ρ is the density of sea water, g is the acceleration of gravity, H_b^2 is the significant wave height at the wave break point, and α_b is the angle of wave incidence at the wave break point. Correlations were performed between the data measured simultaneously in the two regions (in the surf zone and at the mooring site).

The same selected wave parameters (Hs, Tp, and Dir) were correlated with the mean profile. The correlation was also performed with the mean alongshore current velocities considering their directions measured in the surf zone.

3. Results and discussion

3.1. Waves

Figs. 5 and 6 show the time series of Hs (a), Tp (b), and Dir (c) measured by the AWAC in moorings #2 and #4, which covered the current measurement periods from field campaigns #1 to #4. Fig. 7 presents the WW3 model results for the period of May to October, which covers field campaigns #5 and #6.

The field campaigns of current measurements in the surf zone are indicated by the dashed rectangles in Figs. 5, 6, and 7. During the field campaigns, different sea conditions were observed: the significant wave height (Hs) was between 0.92 and 2.8 m; the peak period (Tp) ranged from 4.7 to 16.3 s; and the mean wave direction (Dir) was between 75° (E-NE direction) and 150° (SE-E direction). These directions can be considered as typical and are in agreement with previous studies in the region (Almeida et al., 1999; Strauch et al., 2009).

3.2. Alongshore currents

Four patterns of the mean vertical profile of the current velocities in the surf zone were identified (see Fig. 8): (a) a decreasing vertical profile, i.e., higher velocities at the surface and lower on the bottom; (b) an increasing vertical profile, with lower velocities at the surface than on the bottom; (c) a convex vertical profile, with lower velocities in the middle of the water column; and (d) a concave vertical profile, with lower speeds at the surface and bottom of the water column. The mean alongshore current profiles of types "a" and "d" are considered as typical for this type of environment (Faria et al., 1998; Wang et al., 2002; Zhang and Zou, 2012). The mean profiles with "b" patterns are associated with winds that have a direction contrary to the current, causing a slowdown at the top. The "c" pattern is associated with winds in the same direction as the current, which generates intensification on the surface layer. These patterns indicate the importance of this driving force in the alongshore current dynamics within
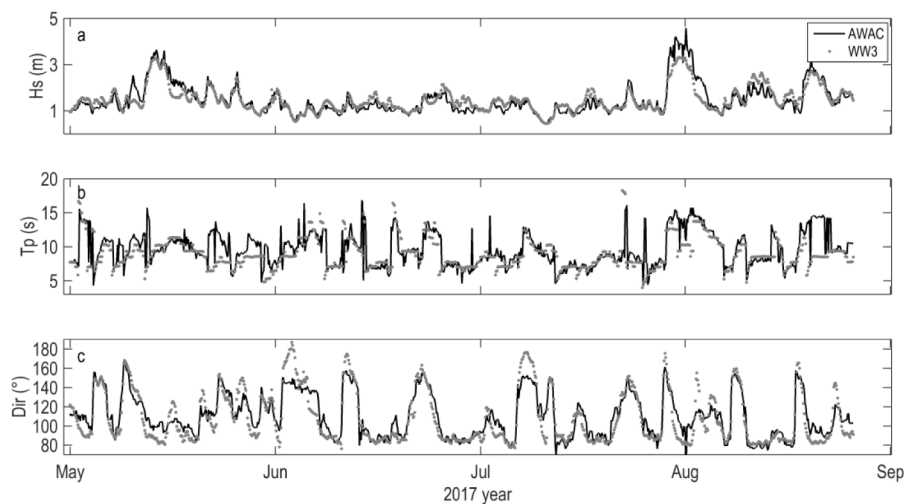
Fig. 4. Validation of AWAC model results (black) using WW3 data (dotted) for all the analyzed parameters (Hs, Tp, Dir) from 2017.
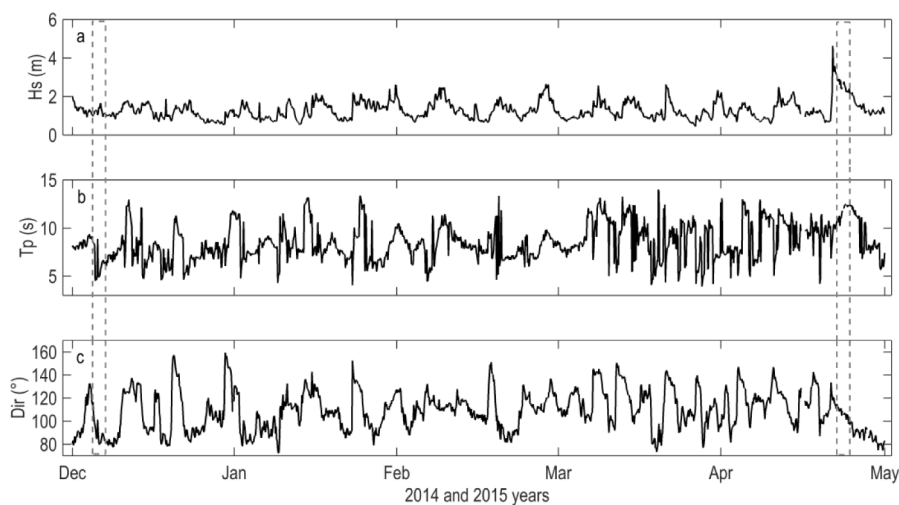
Fig. 5. Time series of the wave parameters recorded by the AWAC between December 2014 and May 2015. (a) significant wave height, (b) peak period, and (c) mean wave direction. Dashed rectangles indicate the periods of the alongshore current measurements during the field campaigns.
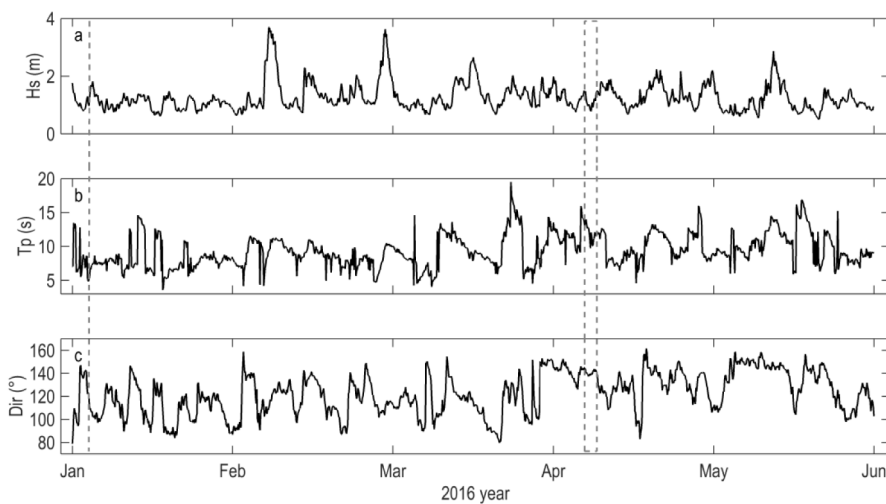
Fig. 6. Time series of the wave parameters recorded by the AWAC between January and June 2016. (a) significant wave height, (b) peak period, and (c) mean wave direction. Dashed rectangles indicate the periods of the alongshore current measurements during the field campaigns.
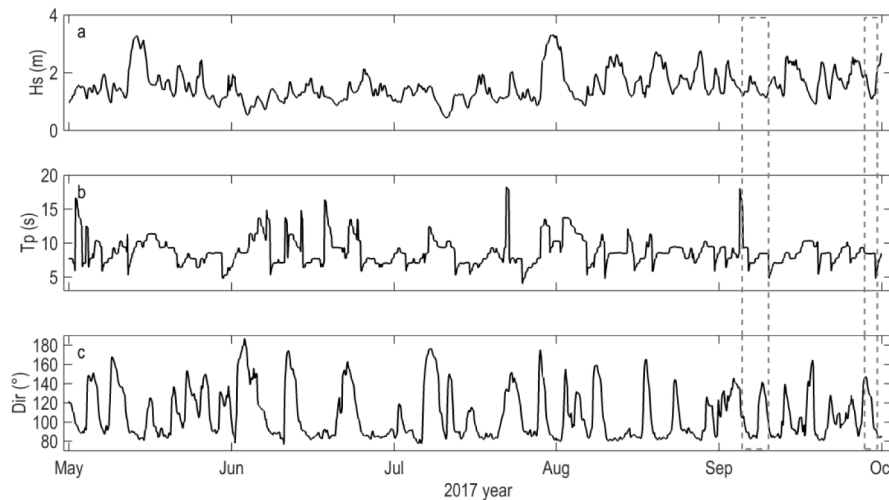
Fig. 7. Time series of the wave parameters generated by the WW3 model between May and October 2017. (a) significant wave height, (b) peak period, and (c) mean wave direction. Dashed rectangles indicate the periods of the alongshore current measurements during the field campaigns.

the surf zone from the beaches on the northern RS coast. The wind stress driving alongshore currents on North American and European beaches is well documented and discussed (Hubertz, 1986; Ruessink et al., 2001). However, field measurements and the following interpretation of the vertical profile behavior have not been greatly explored, even in the global literature.

The field measurement analyses identified a variability in the mean vertical profile of the alongshore currents in this region for the first time. The influence of wind drag on the surface layer was observed, as can be seen in Fig. 8b and c. The wind appears to be responsible for accelerating or slowing the alongshore current in the closest layer to the surface. However, these results disagree with what was proposed by Jung and Toldo (2011), who described only one type of mean profile: higher velocities at the surface, decreasing towards the bottom.

The influence of coastal currents that occur nearshore in circulation within the surf zone can also be excluded. Along the coast of RS, coastal currents on the nearshore are driven by the wind (Zavialov et al., 2002; Costa and Möller, 2011; Andrade et al., 2016). Andrade et al. (2016, 2018), who used the current velocity and sea level data of the same moorings in the present work, indicated that a correlation between local wind, and the currents and the sea level in the nearshore exists.

This variation in the vertical profile of alongshore currents can directly influence the coastal drift transport capacity, since the vertical profile of suspended sediment concentration is also not uniform along the water column (Esteves et al., 2005; Ma, 2003). Therefore, more studies of coastal drift considering the vertical variations of the velocity profile and sediment concentration in the water column should be conducted.

There was no significant influence of the platform pillars on current measurements. A slight change in direction was observed, less than 5°. As the direction of the current was standardized in the present work, for N or S, this did not influence the final results. Previous studies have also found no significant influence from the fishing platform (Jung and Toldo, 2011, 2012). However, in other parts of the world this has been observed, such as at Duck beach, North Carolina (Pianca et al., 2015).

3.3. Waves and currents

Fig. 9 shows the relationship between the current direction data measured at the fishing platform (*x* axis) and the angle of wave incidence (*y* axis). All six field campaigns were taken

into account to compute the angle. Positive angles of incidence correspond to waves with directions greater than 110° (SE), and negative values represent less than 110° (NE).

The yellow and red rectangles in Fig. 9 correspond to the results that agree with the theories of alongshore current formation by the breaking of obliquely angled waves (Komar, 1976; Nielsen, 2009). That means that waves from the south-quadrant (positive angles) induce a northerly current, and north-quadrant waves (negative angles) tend to develop a southward current.

However, the cluster of points in the upper right corner of Fig. 9 represents southerly currents, which are not explained by the theory. Of the total measurements, 17% showed this behavior. In two cases, the incidence angle was inferior to 1°, almost parallel to the coast. In other cases, we found that this has always been observed during bimodal seas, i.e., the coexistence of swells and sea waves. Longitudinal currents directed to the south were observed even in wave conditions with a positive peak direction (S-SE). This process may be related to the distribution of energy in more than one direction in the wave spectrum (Fig. 10), as observed in the behavior described above.

The wind conditions during the measurements of these specific cases (out of the boxes, Fig. 9) were analyzed. Even with winds higher than 4 m/s in the opposite direction, the direction of the longitudinal current did not suffer a significant impact. That is, there was no observed influence of the wind in this process.

Correlation tests were performed between peak wave period data and current intensity and also between wind direction and mean alongshore current, however they were not significant.

Fig. 11 shows the relationship between the significant wave height and the mean current velocity measured in the region between sandbars. A slight tendency of increasing current intensity was noted with increasing wave height. There is a correlation between Hs and the alongshore current intensity, but it was considered weak since R = 0.34.

The comparison between the alongshore current velocity measured in the surf zone and the momentum flux along the coast was calculated using Eq. (1). This equation takes into account the significant wave height and the wave incidence angle at the breaking point. The result pointed to a positive correlation (R = 0.76). This indicates that there is a concordance between the theory of radiation stress by Nielsen (2009) and the region under study.

Fig. 12 shows the comparison between those variables. The alignment of the data points observed is in agreement with the
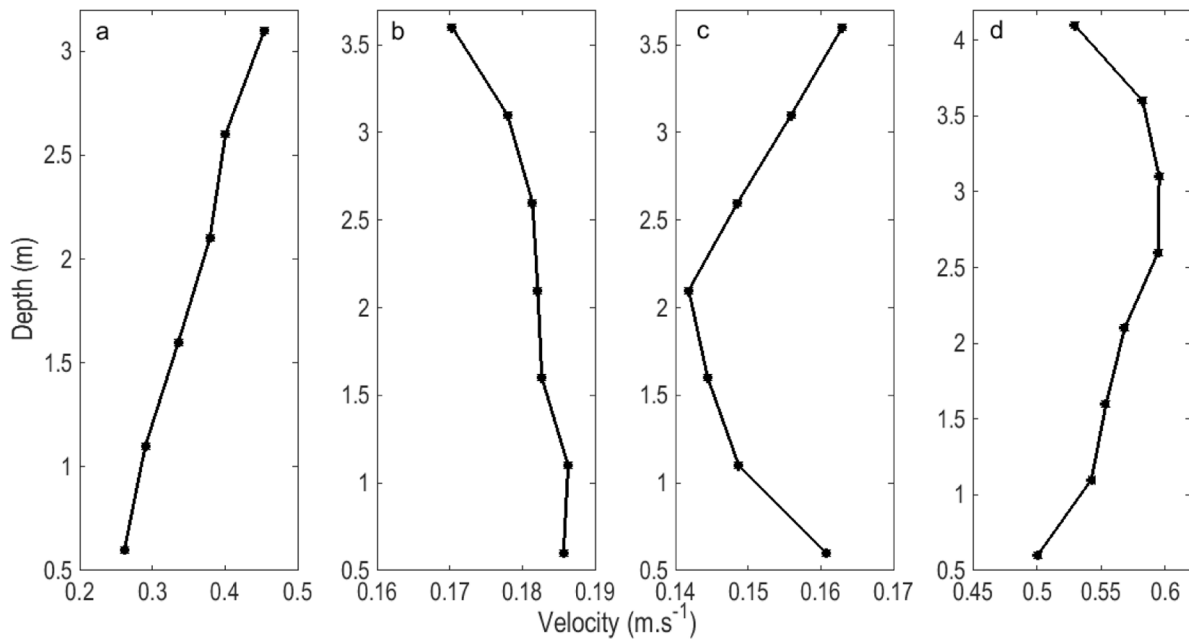
Fig. 8. Four patterns of the mean vertical profile of the alongshore current speed in module. (a) decreasing profile, (b) increasing profile, (c) convex profile, (d) concave profile.
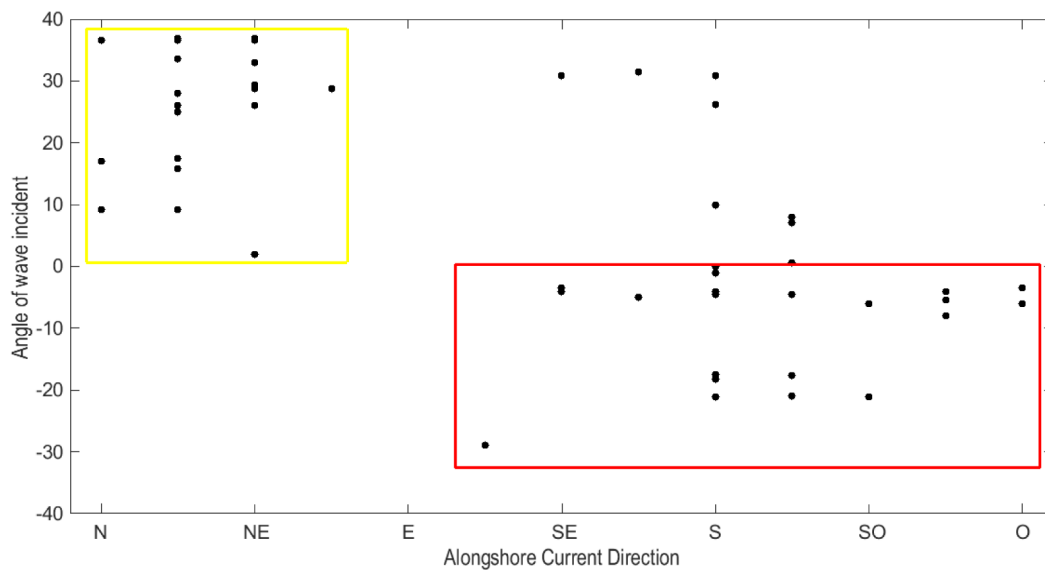
Fig. 9. Correspondence between the angle of wave incidence and the direction of the alongshore current. Positive angles of incidence correspond to waves with directions greater than 110° (SE), and negative values represent less than 110° (NE). (For interpretation of the references to colour in this figure legend, the reader is referred to the web version of this article.)

momentum flow theory. It was also observed that waves with higher heights and/or greater incidence angles develop more intense currents in the surf zone. However, as well as the direct comparison between the wave directions and alongshore currents, some data points (in red, Fig. 12) diverged from what was expected (Komar, 1976; Nielsen, 2009). According to Feddersen (2004), radiation stress fits perfectly in narrow-band conditions of the wave direction spectrum. This could justify the non-aligned data points that are associated with bimodal seas states, i.e., the presence of waves from distinct quadrants (NE and SE), which characterizes a broad-band spectrum.

Based on the results, it was possible to identify a bidirectionality of the currents in the surf zone on the northern RS coast, which was related to the direction of wave incidence, in unimodal sea conditions. Two patterns were described: when

the wave originated from the SE, an alongshore current towards the NE was measured; when waves from the NE occurred, the alongshore current was driven towards the SW. This alongshore current behavior had already been qualitatively described for the region under study in the investigations by Nicolodi et al. (2000), and Jung and Toldo (2012). In these research works, a seasonal pattern was identified in the directions of the alongshore surface current. In the summer and spring months, the flow was towards the SW, while in the winter and autumn, northeasterly currents predominated.

However, the annual bidirectional pattern did not prevail, i.e., the resulting annual coastal drift could be towards the SW or NE. According to Nicolodi et al. (2000), between 1996 and 1997, southwesterly currents were more predominant (62.8%) when compared with northeasterly currents (54.8%). Although, between
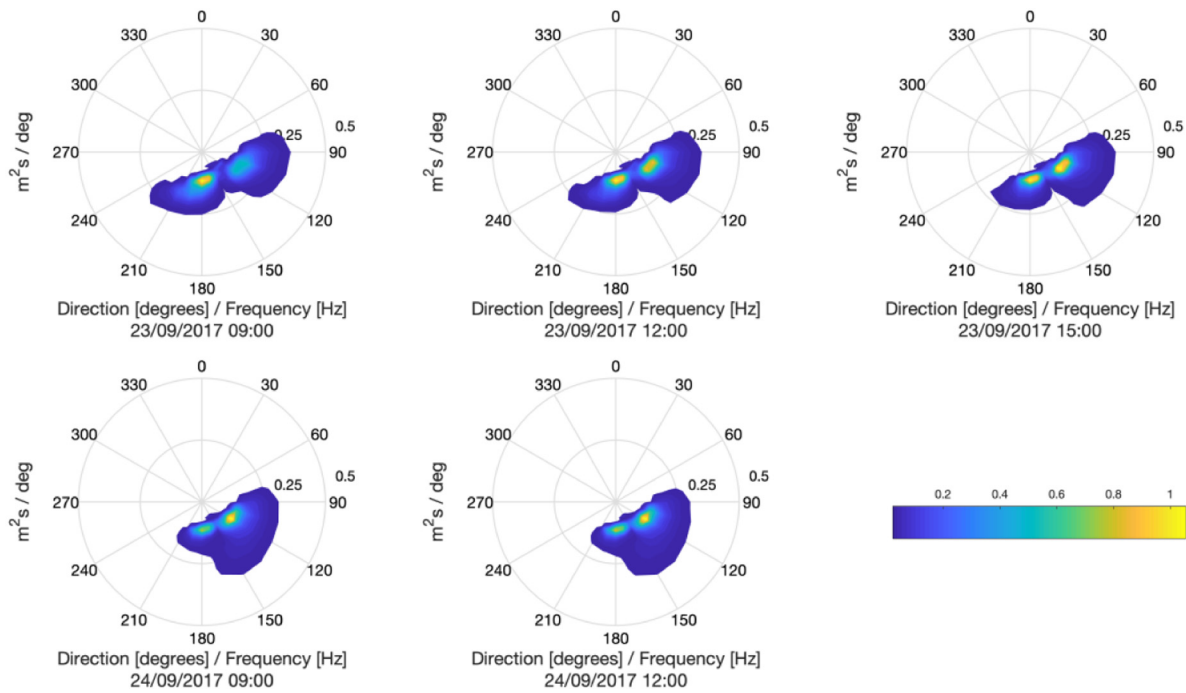
Fig. 10. The two-dimensional spectrum of waves, generated from the WW3 results for September 23 and 24, 2017.
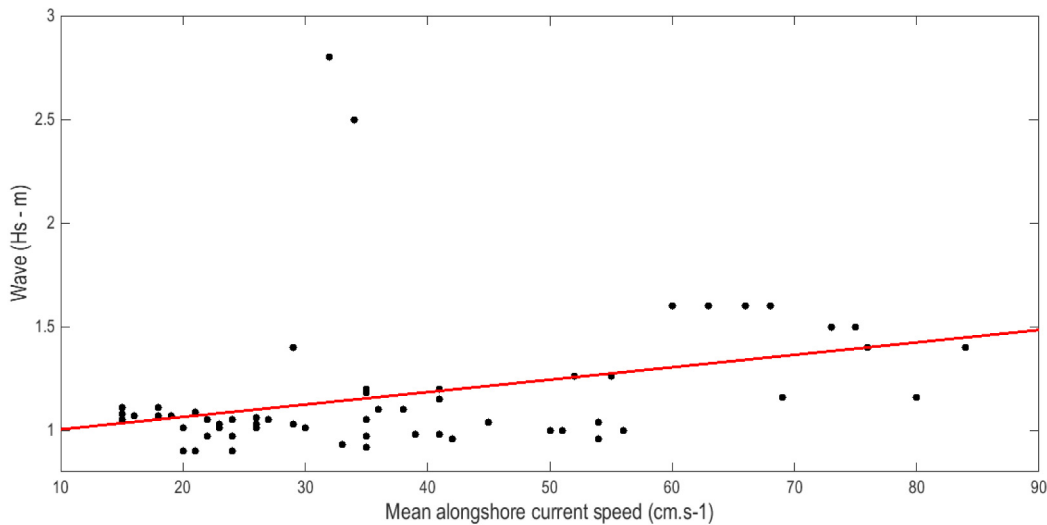
Fig. 11. Correlation between significant wave height (Hs) and intensity of the mean alongshore current in the region between sandbars.

1998 and 1999 there was an inversion of this pattern, which was characterized by a slight prevalence of northeasterly currents in 54% of the analyzed cases.

Nevertheless, the present study quantified the importance of the height and angle of wave incidence in the generation of the alongshore current by calculating the radiation stress. The radiation stress flux is transversal to the movement of wave propagation and can drive an alongshore current (Feddersen, 2004). This flux is characteristic of each environment and can co-exist with tide- and wind-driven currents (Komar, 1976; Nielsen, 2009). This process is responsible for producing an energy vector that drives currents within the surf zone (Davis and FitzGerald, 2009) and is associated with the approaching of waves that are obliquely angled in relation to the coastline. It takes place after the wave-breaking zone and is mainly controlled by the height and angle of wave incidence.

The circulation of currents in the surf zone is a highly dynamic process and is responsible for transporting sediments that were reworked by wave breaking (Hamilton and Ebersole, 2001). Even in a moderate wave energy regime, the direction of the littoral drift is governed by the breaker angle (George et al., 2019). The resulting coastal drift is more efficient when the waves reach a rectilinear or slightly curved coast and with a constant bathymetry on the bottom, such as the northern RS coast (Dillenburg et al., 2004; Toldo et al., 2006a). Coastal drift increases as the wave energy increases, being more pronounced in regions with a small astronomical tide amplitude (also something characteristic of the RS coast), which results in a more continuous and concentrated influence of waves (Siegle and Asp, 2007).

Sediment quantities of scales of millions of m^3 (Lima et al., 2001; Motta et al., 2015; Trombetta et al., 2020) are transported by alongshore currents along great distances on the coast (Araújo and Alfredini, 2001). An example of this process is presented in
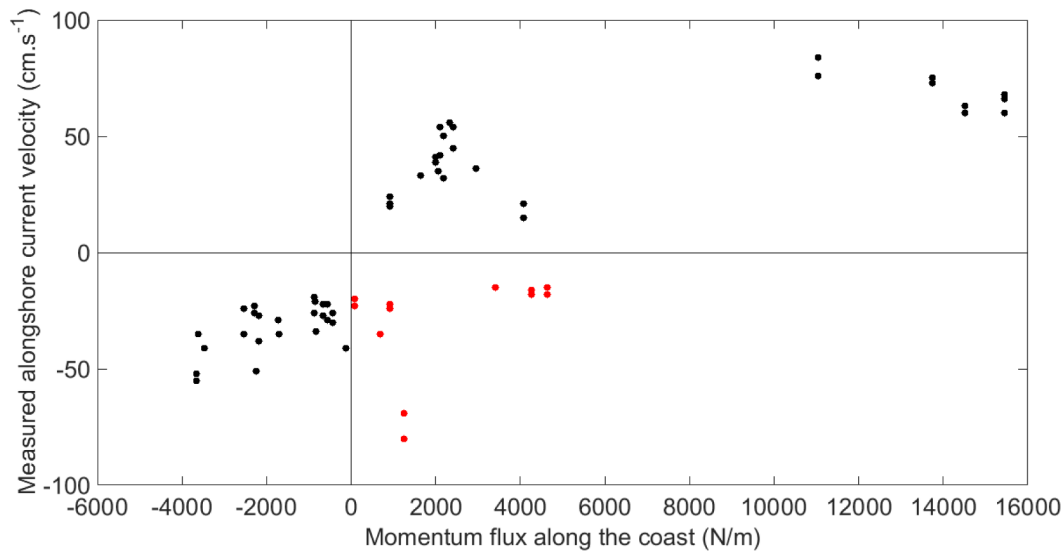
Fig. 12. Relationship between the momentum flux along the coast – calculated using equation 2 – and the velocity of the alongshore current measured in the surf zone. Positive values correspond with fluxes and currents towards the NE, and negative values represent fluxes and currents towards the SW. Red dots represent bimodal sea conditions.

Dillenburg et al. (2020) for a region further south of the study area of the present work. A beach in said region has a sediment deficit caused by a natural interruption of coastal drift, in a region hundreds of kilometers away from the beach that was being eroded. Understanding wave dynamics and their relation with alongshore currents is important for the management of coastal environments, especially in urbanized areas.

4. Conclusions

Direct measurements of the alongshore current concomitant with measurements of the wave parameters on the nearshore were used to study the mechanism of energy flux by radiation stress. The process of generating these currents within the surf zone is driven by the breaking waves that have oblique angles of incidence. In the present work, this process was measured and quantified. The results proved that waves are the main driving force of the alongshore current in the study region.

The alongshore momentum flux calculated had a strong correlation with the intensity and direction of the alongshore current. Furthermore, significant correlations were found between wave height and current intensity, and also between the angle of wave incidence and current direction. Therefore, waves with greater heights and higher incidence angles relative to the beach developed more intense alongshore currents on the northern coast of the state of Rio Grande do Sul (RS).

The wind direction's influence on the alongshore current seems to be restricted to just the surface layer, incapable of reversing the current direction in the water column. In some vertical profiles, wind directions that opposed the current caused a significant decrease in the current velocity from the surface to the middle of the water column. The present authors suggest that future studies seek to quantify the relationship between wind speed and alongshore current.

A pattern was identified in which waves from the SE drive currents towards the NE, and waves from the NE generate fluxes towards the SW (Fig. 13). This behavior was observed by applying unprecedented methodology to measure in field the alongshore currents in the study region.
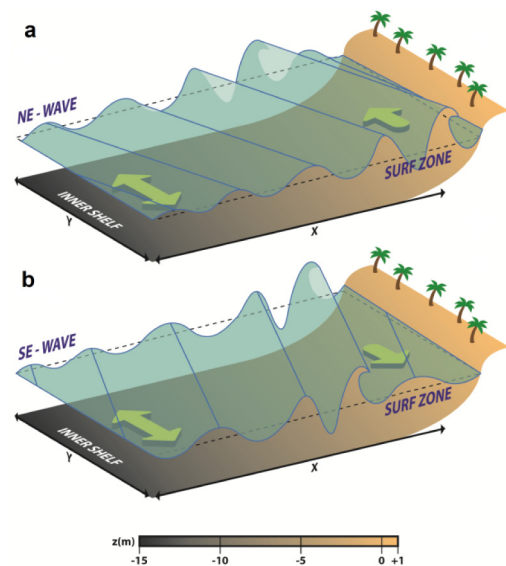
Fig. 13. Scheme of the alongshore current in the surf zone (green arrow) associated with the direction of wave incidence. (a) NE waves and southwesterly alongshore current. (b) SE waves and northeasterly alongshore current. (For interpretation of the references to colour in this figure legend, the reader is referred to the web version of this article.)

Declaration of competing interest

The authors declare that they have no known competing financial interests or personal relationships that could have appeared to influence the work reported in this paper.

Acknowledgments

References

Almeida, L.E.S.B., Rosauro, N.L., Toldo, Jr., E.E., Gruber, NLS., 1999. Avaliação da profundidade de fechamento para o litoral norte do Rio Grande do Sul. In: Anais do SIMPÓSIO BRASILEIRO DE RECURSOS HÍDRICOS, Belo Horizonte, MG. CD-ROM.

Andrade, M.M., Toldo, E.E., Nunes, JCR., 2018. Tidal and subtidal oscillations in a shallow water system in southern Brazil. Braz. J. Oceanogr. 66 (3), 245–254. http://dx.doi.org/10.1590/s1679-87592018017406603.

Andrade, M.M., Toldo, Jr., E.E., Nunes, JCR., 2016. Variabilidade das correntes na plataforma interna ao largo de Tramandaí, RS durante o verão de 2014. Pesquisas Geoci. 43 (3), 289–298. http://dx.doi.org/10.22456/1807-9806.78231.

Araújo, R.N., Alfredini, P., 2001. O Cálculo do Transporte de Sedimentos Litorâneo: Estudo de Caso das Praias de Suarão e Cibratel (Município de Itanhaém, São Paulo). Rev. Bras. Recursos Hídricos 6 (2), 15–28.

Ardhuin, F., Rogers, E., Babanin, A.V., Filipot, J.F., Magne, R., et al., 2010. Semiempirical dissipation source functions for ocean waves. Part I: Definition, calibration, and validation. J. Phys. Oceanogr. 40 (9), 1917–1941. http://dx.doi.org/10.1175/2010JPO4324.1.

Barros, V.R., Grimm, A.M., Doyle, M.E., 2002. Relationship between temperature and circulation in southwestern south america and its influence from el Niño and La Niña events. J. Meteorol. Soc. Japan 80, 21–32.

Calliari, L.J., Guedes, R.M.C., Lélis, R.F., Antiqueira, J.A., Figueiredo, S.A., 2010. Perigos e riscos associados a processos costeiros no Litoral sul do Brasil (RS): uma síntese. Braz. J. Aquat. Sci. Technol. 14 (1), 51–63.

Calliari, L.J., Toldo, Jr., E.E., 2016. Ocean beaches of rio grande do sul. In: Brazilian Beaches Systems, Vol. 17, first ed. Springer, pp. 507–541.

Calliari, L.J., Winterwerp, J.C., Fernandes, E., Cuchiara, D., Vinzon, S.B., Sperle, M., Holland, K.T., 2009. Fine grain sediment transport and deposition in the Patos Lagoon–Cassino beach sedimentary system. Cont. Shelf Res. 29 (3), 515–529.

Cartier, A., Larroudé, P., Héquette, A., 2013. Longshore sediment transport measurements on sandy macrotidal beaches compared with sediment transport formulae. In: Sediment Transport Processes and their Modelling Applications. InTech.

Cavalcanti, I., Kousky, V., 2009. Parte I - Sistemas meteorológicos que afetam o tempo na América do Sul: frentes frias sobre o Brasil. In: Para Entender Tempo E Clima. Oficina de Textos, São Paulo, pp. 135–147.

Chawla, A., Spindler, D.M., Tolman, H.L., 2013. Validation of a thirty year wave hind cast using the climate forecast system reanalysis winds. Ocean Model. 70, 189–206. http://dx.doi.org/10.1016/j.ocemod.2012.07.005.

Costa, R., Möller, Jr., O.O., 2011. Estudo da estrutura e da variabilidade das correntes na área da plataforma interna ao largo de Rio Grande (RS, Brasil), no sudoeste do Atlântico Sul, durante a primavera-verão de 2006–2007. Rev. Gestão Costeira Integrada 11 (3), 273–281.

D'Aquino, CDA., 2004. Calibração e aplicação do modelo numérico Genesis nas praias de Tramandaí e Imbé-RS. In: Programa de Pós-Graduação em Geociências (Dissertation). Universidade Federal do Rio Grande do Sul, RS, Brasil, p. 110.

Davis, Jr., R.A., FitzGerald, D.M., 2009. Beaches and Coasts. John Wiley & Sons, p. 432.

Dillenburg, S.R., Esteves, L.S., Tomazelli, L.J., 2004. A critical evaluation of coastal erosion in Rio Grande do Sul, Southern Brazil. Anais Acad. Bras. Ci. 76 (3), 611–623.

Dillenburg, S.R., Sergio, et al., 2020. Changes in the littoral drift of the Uruguayan coast during the Holocene and its influence in the continuing erosion in southern Brazil. J. Coast. Res. 95, 453–457. http://dx.doi.org/10.2112/SI95-088.1.

Durrant, T., Greenslade, D., Hemar, M., Trenham, C., 2014. A Global Hindcast Focussed on the Central and South Pacific. CAWCR Technical Report No. 70, p. 46.

Esteves, L.S., Williams, J.J., Lisniowski, M.A., Perotto, H., 2005. Caracterização do perfil vertical da concentração de sedimentos transportados na zona de surfe. In: X Congresso da Associação Brasileira de Estudos do Quaternário - Abequa. Anais... Guarapari/ES.

Faria, A.F., Thornton, E.B., Stanton, T.P., Soares, C.K., Lippmann, T.C., 1998. Vertical profiles of longshore currents and related bed shear stress and bottom roughness. J. Geophys. Res. Oceans 103 (C2), 3217–3232.

Feddersen, F., 2004. Effect of wave directional spread on the radiation stress: comparing theory and observations. Coast. Eng. 51 (5–6), 473–481.

Fiore, M.M.E., D'onofrio, E.E., Pousa, J.L., 2009. Storm surges and coastal impacts at Mar del Plata, Argentina. Cont. Shelf Res. 29 (14), 1643–1649.

George, J., Kumar, V.S., Victor, G., Gowthaman, R., 2019. Variability of the local wave regime and the wave-induced sediment transport along the Ganpatipule coast, eastern Arabian Sea. Reg. Stud. Mar. Sci. 31, 100759.

Germani, Y.F., Figueiredo, S.A., Calliari, L.J., Tagliani, CRA., 2015. Vulnerabilidade costeira e perda de ambientes devido à elevação do nível do mar no litoral sul do Rio Grande do Sul. J. Integr. Coastal Zone Manag. 15 (1).

Guimarães, P.V., Farina, L., Toldo, E.E., 2015. Analysis of extreme wave events on the southern coast of Brazil. Nat. Hazards Earth Syst. Sci. 14 (12), 3195–3205. http://dx.doi.org/10.5194/nhess-14-3195-2014.

Hamilton, D.G., Ebersole, B.A., 2001. Establishing uniform longshore currents in a large-scale sediment transport facility. Coast. Eng. 42 (3), 199–218.

Hartmann, C., 1996. Dinâmica, Distribuição e Composição do Material em Suspensão na Região Sul da Laguna dos Patos, RS (Tese). UFRGS, Porto Alegre, RS, Brazil.

Hasselmann, S., Hasselmann, K., Allender, J.H., Barnett, T.P., 1985. Computations and parameterizations of the nonlinear energy transfer in a gravity-wave specturm. Part II: Parameterizations of the nonlinear energy transfer for application in wave models. J. Phys. Oceanogr. 15 (11), 1378–1391.

Holthuijsen, L.H., 2010. Waves in Oceanic and Coastal Waters. Cambridge University Press.

Hubertz, J.M., 1986. Observations of local wind effects on alongshore currents. Coast. Eng. 10, 275–288.

Jung, G.B., Toldo, E.E., 2011. Longshore current vertical profile on a dissipative beach. Rev. Bras. Geofís. 29 (4), 691–702.

Jung, G.B., Toldo, E.E., 2012. Análise qualitativa da direção da corrente longitudinal entre 2004 e 2008 na Praia de Tramandaí, RS, Brasil. Rev. Bras. Geomorfol. 13 (1).

Kalnay, E., Kanamitsu, M., Kistler, R., Collins, W., Deaven, D., Gandin, L., et al., 1996. The NCEP/NCAR 40-year reanalysis project. Bull. Am. Meteorol. Soc. 77 (3), 437–472.

Komar, P.D., 1976. Beach Process and Sedimentation. Prentice Hall, p. 429.

Lélis, R.J., Calliari, L.J., 2003. Variabilidade da linha de costa oceânica adjacente às principais desembocaduras do Rio Grande do Sul, Brasil. In: IX Congresso da Associação Brasileira de Estudos do Quaternário - Abequa. Anais. Recife/PE.

Lima, S.F., Almeida, L.E., Toldo, Jr., E.E., 2001. Estimativa da capacidade de transporte longitudinal de sedimentos a partir de dados de ondas para a costa do Rio Grande do Sul. Pesquisas Geoci. 28 (2), 99–107.

Longuet-Higgins, M.S., 1970. Longshore currents generated by obliquely incident sea waves: 1. J. Geophys. Res. 75 (33), 6778–6789.

Ma, T.T., 2003. Quantificação do transporte longitudinal a partir de dados de concentração de sedimentos em suspensão, Tramandaí-RS (Dissertation). Universidade Federal do Rio Grande do Sul, Porto Alegre, RS, Brasil, p. 72.

Mawdsley, R.J., Haigh, I.D., Wells, N.C., 2014. Global changes in mean tidal high water, low water and range. J. Coast. Res. 70 (1), 343–348.

Melo, E., Hammes, G., Franco, D., Romeu, MAR., 2008. Avaliação de desempenho do modelo WW3 em Santa Catarina. Report Laboratório de Hidráulica Marítima, UFSC.

Motta, V.F., 1964. Resultados de algumas medições de transporte litorâneo em modelo costeiro esquemático. Report n. F1257, Instituto de Pesquisas Hidráulicas – UFRGS, Porto Alegre, p. 46.

Motta, V.F., 1967. Estudo em modelo reduzido para a regularização da embocadura lagunar de Tramandaí/RS. Report. Rio de Janeiro: S. N., p. 69.

Motta, L.M., Toldo, E.E., Almeida, L.E., Nunes, JCR., 2015. Sandy sediment budget of the midcoast of Rio Grande do Sul, Brazil. J. Mar. Res. 73 (3–4), 49–69.

Neves Filho, SC., 1992. Variação da Maré Meteorológica no Litoral Sudeste do Brasil: 1965–1986. Engenharia Costeira e Oceanográfica do Programa de Engenharia Oceânica da COPPE/UFRJ (Dissertation), Rio de Janeiro, Brasil.

Nicolodi, J.L., Toldo, Jr., E.E., Gruber, NLS., 2000. Análise da Direcionalidade das Correntes Litorâneas no Litoral Norte do Rio Grande do Sul. In: XIII Semana Nacional de Oceanografia, 2000, Itajaí, SC. Anais do XIII SNO. Universidade do Vale do Itajaí, pp. 461–463.

Nielsen, P., 2009. Coastal and Estuarine Processes, Vol. 29. World Scientific Publishing Company.

NORTEK, 2013. Comprehensive Manual. Nortek As., p. 138.

PBMC, 2016. Impacto, vulnerabilidade e adaptação das cidades costeiras brasileiras às mudanças climáticas: Relatório Especial do Painel Brasileiro de Mudanças Climáticas [Marengo, JA, Scarano FR]. COPPE - UFRJ, Rio de Janeiro, Brasil, ISBN: 978-85-285-0345-6, p. 184.

Perignon, Y., 2017. Assessing accuracy in the estimation of spectral content in wave energy resource on the French Atlantic test site SEMREV. Renew. Energy (114), 145–153. http://dx.doi.org/10.1016/j.renene.2017.02.086.

Pianca, C., Holman, R., Siegle, E., 2015. Shoreline variability from days to decades: Results of long-term video imaging. J. Geophys. Res. Oceans 120 (3), 2159–2178. http://dx.doi.org/10.1002/2014JC010329.

Pilkey, O.H., Cooper, JAG., 2014. Are natural beaches facing extinction? J. Coast. Res. 70, 431–436. http://dx.doi.org/10.2112/SI70-073.1.

Piola, A.R., Matano, R.P., Palma, E., Möller, O.O., Campos, E.J., 2005. The influence of the plata river discharge on the western South Atlantic Shelf. Geophys. Res. Lett. (32), 10–29.

Pitombeira, E.S., 1975. Estimativa do volume anual de transporte litorâneo na costa do Rio Grande do Sul (Dissertation). Instituto de Pesquisas Hidráulicas (IPH), Universidade Federal do Rio Grande do Sul (UFRGS, Porto Alegre, Brasil, p. 98.

Rascle, N., Ardhuin, F., 2013. A global wave parameter database for geophysical applications. Part 2: Model validation with improved source term parameterization. Ocean Model. (70), 174–188. http://dx.doi.org/10.1016/j.ocemod.2012.12.001.

Roland, A., 2008. Spectral Wave Modelling on Unstructured Meshes (Ph.D. thesis). Institut fur Wasserbau und Wasserwirtschaft.

Ruessink, B.G., Miles, J.R., Feddersen, F., Guza, R.T., Elgar, S., 2001. Modeling the alongshore current on barred beaches. J. Geophys. Res. 106, 451–463.

Schossler, V., Toldo, Jr., E.E., Dani, N., 2017. Morfodinâmica da desembocadura da Lagoa do Peixe, litoral sul do Brasil. Pesquisas Geoci. 44 (1), 25–39.

Siegle, E., Asp, N.E., 2007. Wave refraction and longshore transport patterns along the southern Santa Catarina coast. Braz. J. Oceanogr. 55 (2), 109–120.

Silva, A.F., Toldo, Jr., E.E., 2017. Morfodinâmica da desembocadura da Lagoa de Tramandaí (RS, Brasil). Pesquisas Geoci. 44 (1), 155–166.

Sprovieri, F.C., 2018. Clima de Ondas, Potencial Energético e Transporte de Sedimentos no Litoral Norte do Rio Grande do Sul. In: Programa de Pós-Graduação em Geociências (Tese). Universidade Federal do Rio Grande do Sul, RS, Brasil, p. 142.

Strauch, J.C., Cuchiara, D.C., Toldo, Jr., E.E., 2009. O Padrão das Ondas de Verão e Outono no Litoral Sul e Norte do Rio Grande do Sul. Rev. Bras. Recursos Hídricos 14-4, 29–37.

Toldo, E.E., Dillenburg, S.R., Almeida, L.E.S.B., Tabajara, L.L., Martins, R., Cunha, LOBP., 1993. Parâmetros morfométricos da Praia de Imbé, RS. Pesquisas 20 (1), 27–32.

Toldo, Jr., E.E., Almeida, LESB., 2003. A linha d'água como indicadora da posição da linha de praia. In: IX CONGRESSO DA ASSOCIAçÃO BRASILEIRA DE ESTUDOS DO QUATERNÁRIO - Abequa. Anais. Recife/PE.

Toldo, Jr., E.E., Almeida, L.E.S.B., Nicolodi, J.L., Absalonsen, L., Gruber, NSL., 2006b. O Controle da Deriva Litorânea no Desenvolvimento do Campo de Dunas e da Antepraia no Litoral Médio do Rio Grande do Sul. Pesquisas Geoci. 33 (2), 35–42.

Toldo, Jr., E.E., Nicolodi, J.L., Almeida, L.E.S.B., Corrêa, I.C.S., Esteves, L.S., 2006a. Coastal dunes and shoreface width as a function of longshore transport. In: SI 39 (Proceedings of the 8th International Coastal Symposium), ItajaÍ, SC, Brazil. J. Coast. Res. (ISSN: 0749-0208) 390–394.

Tolman, H.L., 2003. Treatment of unresolved islands and ice in wind wave models. Ocean Model. 5, 219–231.

Tolman, H.L., 2009. User Manual and System Documentation of WAVEWATCH-III. Technical report, NOAA/NWS/NCEP/OMB.

Tomazelli, L., Villwock, J., 1992. Considerações sobre o ambiente praial e a deriva litorânea de sedimentos ao longo do litoral norte do Rio Grande do Sul, Brasil. Pesquisas Geoci. 19 (1), 3–12.

Torres-Freyermuth, A., Puleo, J.A., DiCosmo, N., Allende-Arandía, M.E., Chardón-Maldonado, P., et al., 2017. Nearshore circulation on a sea breeze dominated beach during intense wind events. Cont. Shelf Res. 151, 40–52.

Trombetta, T.B., Marques, W.C., Guimarães, R.C., Costi, J., 2020. An overview of longshore sediment transport on the Brazilian coast. Reg. Stud. Mar. Sci. 101099.

U. S. Army Coastal Engineering Research Center/CERC, 1984. Shore Protection Manual, Vol. I, fourth ed. U. S. A. Gorvernment Print Office, Washington, p. 208.

van Rijn, L., 1993. Principles of Sediment Transport in Rivers, Estuaries and Coastal Seas. pp. 1–17, Princ. Sediment Transp. Rivers, Estuaries Coast. Seas.

Villas-Boas, A.B., Ardhuin, F., Ayet, A., Bourassa, M.A., Chapron, B., Brandt, P., et al., 2019. Integrated observations and modeling of global winds, currents, and waves: requirements and challenges for the next decade. Front. Mar. Sci. 6, 425.

Wang, P., Ebersole, B.A., Smith, E.R., Johnson, B.D., 2002. Temporal and spatial variations of surf-zone currents and suspended sediment concentration. Coast. Eng. 46 (3), 175–211.

Zavialov, P., Möller, Jr., O.O., Campos, E., 2002. First direct measurements of currents on the continental shelf of Southern Brazil. Cont. Shelf Res. 22, 1975–1986.

Zhang, Z.W., Zou, Z.L., 2012. Vertical distribution of longshore currents over plane and barred beaches. J. Hydrodyn. 24 (5), 718–728.